Cell Reports

Article

Loss of 4E-BP converts cerebellar long-term depression to long-term potentiation

Graphical abstract

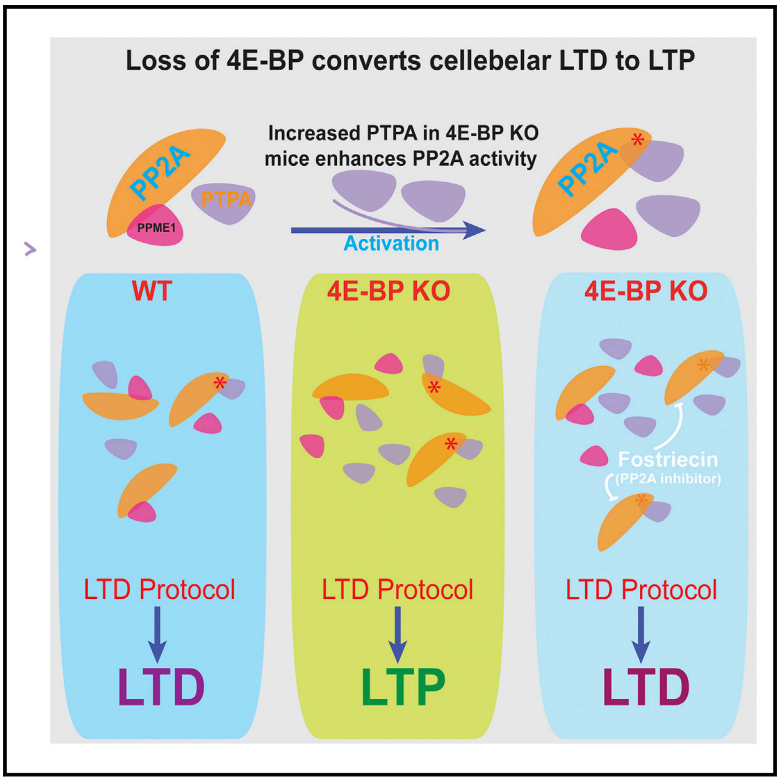

Authors

Natasha Saviuk, Yumaine Chong, Peng Wang, ..., Nahum Sonenberg, Ellis Cooper, A. Pejmun Haghighi

Correspondence

ellis.cooper@mcgill.ca (E.C.), phaghighi@buckinstitute.org (A.P.H.)

In brief

Saviuk et al. demonstrate that in 4E-BP1/2 KO mice, cerebellar LTD is converted to LTP. This is due to enhanced PP2A activity, as treatment with PP2A inhibitors restores LTD. 4E-BP is, therefore, required for ensuring the appropriate phosphatase/kinase balance and establishing normal synaptic plasticity in the cerebellum.

Highlights

- In 4E-BP1/2 KO mice, cerebellar LTD is converted to LTD
- Basal synaptic function in 4E-BP1/2 KO mice is normal
- Expression of PTPA, PP2A activator, is enhanced in 4E-BP1/2 KO mice
- Pharmacological inhibition of PP2A restores LTD in 4E-BP1/2 KO mice

Saviuk et al., 2022, Cell Reports *39*, 110911
June 7, 2022
https://doi.org/10.1016/j.celrep.2022.110911

CellPress

Cell Reports

CellPress
OPEN ACCESS

Article

Loss of 4E-BP converts cerebellar long-term depression to long-term potentiation

Natasha Saviuk,[1,2] Yumaine Chong,[1,2] Peng Wang,[3] Sara Bermudez,[3] Zhe Zhao,[1] Arjun A. Bhaskaran,[1,4] Derek Bowie,[1,4] Nahum Sonenberg,[3] Ellis Cooper,[1,2,*] and A. Pejmun Haghighi[1,2,5,6,*]

[1]Integrated Program in Neuroscience, McGill University, Montréal, QC, Canada
[2]Department of Physiology, McGill University, Montréal, QC, Canada
[3]Biochemistry, McGill University, Montréal, QC, Canada
[4]Pharmacology and Therapeutics, McGill University, Montréal, QC, Canada
[5]Buck Institute for Research on Aging, Novato, CA, USA
[6]Lead contact
*Correspondence: ellis.cooper@mcgill.ca (E.C.), phaghighi@buckinstitute.org (A.P.H.)
https://doi.org/10.1016/j.celrep.2022.110911

SUMMARY

Genetic perturbances in translational regulation result in defects in cerebellar motor learning; however, little is known about the role of translational mechanisms in the regulation of cerebellar plasticity. We show that genetic removal of 4E-BP, a translational suppressor and target of mammalian target of rapamycin complex 1, results in a striking change in cerebellar synaptic plasticity. We find that cerebellar long-term depression (LTD) at parallel fiber-Purkinje cell synapses is converted to long-term potentiation in 4E-BP knockout mice. Biochemical and pharmacological experiments suggest that increased phosphatase activity largely accounts for the defects in LTD. Our results point to a model in which translational regulation through the action of 4E-BP plays a critical role in establishing the appropriate kinase/phosphatase balance required for normal synaptic plasticity in the cerebellum.

INTRODUCTION

While mounting evidence points to a prominent role for mammalian target of rapamycin complex 1 (mTORC1)-dependent translational mechanisms in the regulation of cerebellar-dependent motor learning (Banko et al., 2007; Cupolillo et al., 2016; Kloth et al., 2015; Tsai et al., 2012), little is known about how these translational pathways influence long-term synaptic plasticity in the cerebellum. Rapid cerebellar-dependent motor learning correlates positively with the induction of long-term synaptic plasticity of parallel fiber (PF)-Purkinje cell (PC) synapses in the cerebellar cortex (Aiba et al., 1994; De Zeeuw et al., 1998; Feil et al., 2003; Hansel et al., 2006; Kakegawa et al., 2008; Kashiwabuchi et al., 1995; Miyata et al., 2001; Yuzaki, 2013). Moreover, pharmacological inhibition of protein synthesis and mRNA translation prevents long-term depression (LTD) of glutamatergic currents on isolated Purkinje neurons (Linden, 1996) and PF-PC synapses in acute cerebellar slices (Karachot et al., 2001); this suggests there is a link between regulation of mRNA translation and the kinase/phosphatase processes involved in the induction of synaptic plasticity at PF-PC synapses.

Current models propose that the induction of long-term potentiation (LTP) and LTD at PF-PC synapses occurs through independent, competing processes driven by increased kinase or enhanced phosphatase activity, respectively, with each being regulated by a distinct sensitivity for calcium (Kawaguchi and Hirano, 2013). LTD occurs at PF-PC synapses when parallel synapses are co-activated with climbing fiber (CF) synapses and requires the activation of PKC (Leitges et al., 2004; Linden and Connor, 1991), cGKI (Feil et al., 2003), alpha CaMKII (Hansel et al., 2006), and beta CaMKII (van Woerden et al., 2009). On the other hand, LTP occurs at PF-PC synapses when PFs are activated at low frequency without co-activation of CF synapses (Lev-Ram et al., 2002). The kinases involved in LTD are not required to induce LTP (Belmeguenai and Hansel, 2005; Hansel et al., 2006; Kakegawa and Yuzaki, 2005); instead, the induction of LTP requires the activation of PP1, PP2A, and calcineurin (PP2B) (Belmeguenai and Hansel, 2005). The selective deletion of PP2B abolishes LTP at PF-PC synapses (Schonewille et al., 2010), whereas the induction of LTD is unaffected.

While the critical importance of the kinase/phosphatase balance for long-term plasticity at PF-PC synapses is well established, the way translational mechanisms establish and maintain this balance at PF synapses is not known. Cap-dependent translation initiation depends critically on the formation of the cap-binding complex that includes three eukaryotic initiation factors, eIF4E, eIF4G, and eIF4A (Sonenberg et al., 1979). 4E-BPs compete with eIF4G for binding to eIF4E and thereby impair eIF4F formation and translation initiation. The inhibitory action of 4E-BP is regulated through phosphorylation by mTORC1, which leads to dissociation of 4E-BP from eIF4E (Gingras et al., 1999; Richter and Sonenberg, 2005). Interestingly, 4E-BP mutant mice are homozygous viable and thus have been used as a model for investigating the role of mTORC1-dependent translational

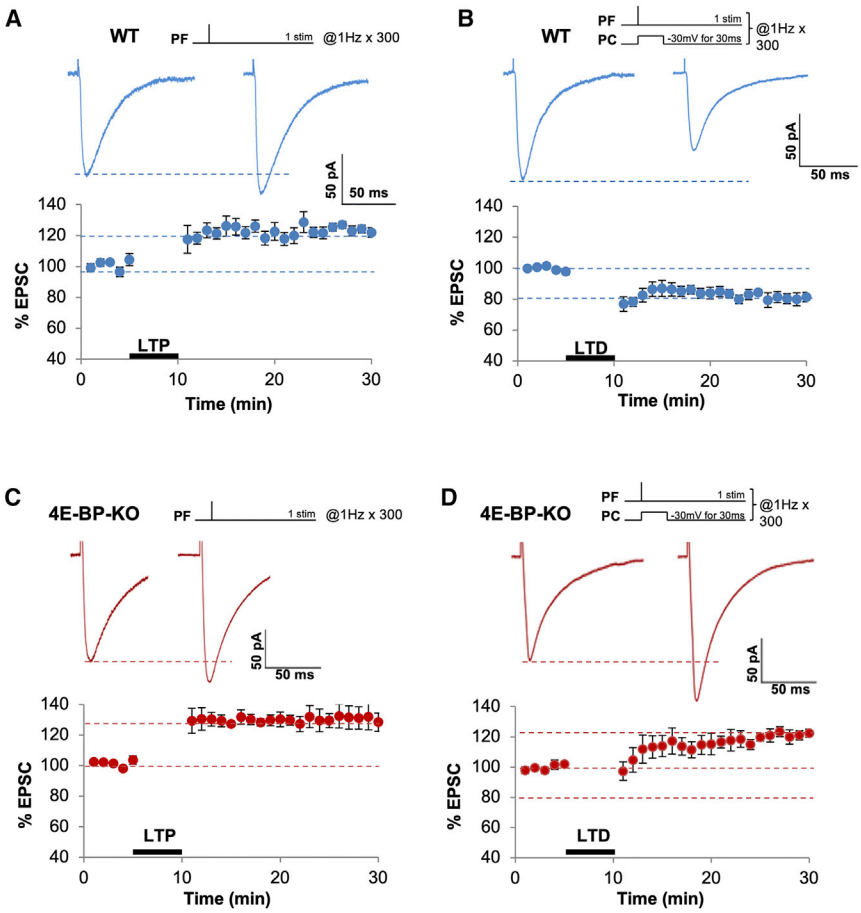

Figure 1. Genetic deletion of 4E-BP1/2 reverses the polarity of PF-PC LTD

(A) In WT cerebellar slices, PF stimulation alone at 1 Hz for 5 min, without conjunctive depolarization, potentiates PF-EPSCs (124.30% ± 2.61%, t = 25–30 min, n = 5, paired Student's t test p = 0.00043).

(B) In WT cerebellar slices, pairing PF stimulation at 1 Hz for 5 min with a depolarizing voltage step to the Purkinje cell body to −30 mV for 30 ms depresses PF-EPSCs to ~80% of baseline (79.09% ± 3.76%, t = 25–30 min, n = 4, paired Student's t test p = 0.007).

(C) In cerebella from 4E-BP-KO mice, PF stimulation alone potentiated PF-EPSCs (125.24% ± 4.78%, t = 25–30 min, n = 4, paired Student's t test p = 0.012), comparably to WTs (Mann-Whitney U test p = 0.39).

(D) In acute cerebellar slices from 4E-BP-KO mice, the LTD induction protocol (pairing PF stimulation at 1 Hz for 5 min with a depolarizing voltage step to the Purkinje cell body to −30 mV for 30 ms depresses) potentiates PF-PC synapses to approximately 120% of baseline (121.52% ± 2.98%, t = 25–30 min, n = 5, paired Student's t test p = 0.00075), significantly different from WTs (Mann-Whitney U test p < 0.00001). All error bars are standard error of the mean.

mechanisms that participate in the regulation of different aspects of synaptic growth, function, and plasticity (Aguilar-Valles et al., 2015; Banko et al., 2005, 2007; Chong et al., 2018; Ran et al., 2009, 2013). We, therefore, asked whether genetic removal of 4E-BP (4E-BP1 and 4E-BP2) would interfere with cerebellar synaptic plasticity.

Our electrophysiological examination demonstrates that loss of 4E-BP leads to a severe impairment of postsynaptic LTD at PF-PC synapses without any effect on LTP. Our pharmacological and biochemical analysis suggests that increased PP2A activity underlies the defect in LTD in 4E-BP KO mice. These results provide mechanistic insight into the regulation of cerebellar synaptic plasticity by demonstrating a critical role for 4E-BP in the phosphatase/kinase balance needed for appropriate induction of LTD in the cerebellum.

RESULTS

Cerebellar LTD at PF-PC synapses is impaired in 4E-BP1/2-KO mice

In acute cerebellar slices from P21-30 wild-type (WT) mice, stimulation of PFs at 1 Hz for 5 min led to potentiation of excitatory postsynaptic currents (EPSCs) recorded from PCs (124.30% ± 2.61%, t = 25–30 min, n = 5), indicating the induction of postsynaptic LTP (Figure 1A). On the other hand, pairing the same stimulation protocol together with a 30-ms step depolarization of the postsynaptic PCs to −30 mV repeatedly at 1 Hz for 5 min depressed EPSCs (79.09% ± 3.76%, t = 25–30 min, n = 4), indicating the induction of LTD (Figure 1B).

In order to interrogate the role of mTORC1-dependent mechanisms in the regulation of cerebellar long-term plasticity, we investigated mice with deletions in both 4E-BP1 and 4E-BP2 genes; while 4E-BP2 is the primary 4E-BP isoform in the central nervous system (Bidinosti et al., 2010; Tsukiyama-Kohara et al., 2001), we previously found that mRNA and protein for 4E-BP1 could be detected in cerebellar cortex (Chong et al., 2018) (also see Figure 4 in this manuscript). Here onward, we will refer to these mice as 4E-BP-KO. Using cerebellar slices from 4E-BP-KO mice at P21-30, we found that LTP at PF-PC synapses is intact (125.24% ± 4.78%, t = 25–30 min, n = 4, Figure 1C). Strikingly, however, we found that pairing PF stimulation with PC depolarization led to LTP instead of LTD at PF-PC synapses (121.52% ± 2.98%, t = 25–30 min, n = 5, Figure 1D).

We next investigated whether this unexpected change in plasticity gain was associated with detectable changes in gross cerebellar cortex morphology or basic electrophysiological properties at CF-PC or PF-PC synapses. In 4E-BP-KO mice, the size and density of PCs in the cerebellar cortex remained indistinguishable from those in WT mice (Figures S1A–S1C). We did not detect any significant differences in the intrinsic firing frequency of PCs in acute slices (Figure S1D), nor in the refinement of CF axons innervating PCs (Figure S1E). Moreover, CF-PC EPSCs and paired-pulse ratios in 4E-BP KO mice were indistinguishable from those in WT mice (Figures S1F and 1G).

Furthermore, there was no statistical difference in paired-pulse ratios at PF-PC synapses between WT and 4E-BP-KO mice (Figure S1H), ruling out a change in PF release probability in 4E-BP-KO mice. In addition, we compared PF-PC EPSPs paired-pulse ratio before and after applying the LTD-inducing protocol and did not detect any difference in slices from WT and 4E-BP mice (Figure S1I); this suggests that the LTD induction protocol did not differentially affected PF release probability in 4E-BP-KOs.

Based on these results, it is unlikely that gross changes in the development of the cerebellar cortex, defects in basic firing properties of PCs, or defects in electrophysiological properties of PF-PC and CF-PC synapses are responsible for the conversion of LTD to LTP in 4E-BP KO mice.

Deletion of 4E-BP does not affect calcium influx in PCs

Our electrophysiological analysis demonstrates that a stimulation protocol that produces LTD in WT cerebellar slices produces LTP at PF-PC synapses in 4E-BP-KO mice. Induction of PF-PC LTD requires large calcium elevations in PCs. Conversely, PF-PC LTP is induced with lower levels of intracellular calcium (Coesmans et al., 2004), and consequently, in the absence of conjunctive depolarization, PF-PC synapses undergo LTP. This raises the possibility that if calcium influx were impaired during conjunctive stimulation in 4E-BP-KOs, PF-PC synapses would undergo LTP instead of LTD. To test this possibility, we measured depolarization-induced rise in intracellular calcium with the calcium indicator Oregon-Green-BAPTA-1 following standard protocols. We did not find any differences in the average size of calcium transients in PCs in WT and 4E-BP-KO mice, indicating that deletion of 4E-BP did not affect calcium influx through voltage-gated calcium channels (Figure 2A).

In addition, to test further the possibility that conjunctive depolarization in 4E-BP-KO cerebellar slices was somehow ineffective, we used an alternative protocol that does not induce LTP in the absence of the paired conjunctive stimulation (Shin and Linden, 2005). In this LTD-inducing protocol, PFs are stimulated with 5 trains at 100 Hz accompanied by 100-ms-long depolarization of the PC to 0 mV, repeated 30 times at 2-s intervals (Shin and Linden, 2005). In WT cerebellar slices, this protocol depressed PF-PC EPSCs (79.05% ± 2.72%, t = 21–25 min, n = 6) and produced LTD (Figure 2A). In contrast, in 4E-BP-KOs, this protocol potentiated PF-EPSCs (119.442% ± 5.73%, t = 21–25 min, n = 6) and produced LTP (Figure 2B). In both WT and 4E-BP-KO slices, omitting the conjunctive depolarization did not induce any significant change in EPSCs from baseline (Figures S2A and S2B), precluding the possibility that any LTD stimulation protocol without PC depolarization would trigger LTP.

The switch in PF-PC synaptic plasticity from LTD to LTP in 4E-BP-KO depends on mRNA translation

A rate-limiting step in translation initiation is the binding of the eukaryotic initiation factor 4E (eIF4E) to the 5′ cap structure of the mRNA (Gingras et al., 1999; Sonenberg and Hinnebusch, 2009). Availability of eIF4E is largely regulated through the inhibitory action of 4E-BP; mTORC1 promotes translation initiation in part by phosphorylating 4E-BP and preventing it from binding to and inhibiting eIF4E (Haghighat et al., 1995; Mader et al., 1995; Marcotrigiano et al., 1999; Pause et al., 1994). If the change in plasticity gain at PF-PC synapses in 4E-BP mutant cerebellar slices is due to unregulated cap-dependent translation, it should be possible to suppress it through pharmacological inhibition of translation initiation. To test this idea, we perfused 4EGI-1, a potent inhibitor that specifically blocks eIF4E/eIF4G interaction and translation initiation, into the bath for 10 min prior to the induction of LTD (Gkogkas et al., 2013). 4EGI-1 prevented LTD induction at PF-PC synapses (98.03% ± 5.38%, t = 26–30 min, n = 5, p = 0.2675) in WT mice (Figure 3A). Similarly, in 4E-BP-KO cerebellar slices treated with 4EGI-1, LTD-inducing stimuli did not produce any significant potentiation or depression of EPSCs at PF-PC synapses (97.73% ± 3.50%, t = 26–30 min, n = 6, p = 0.46) (Figure 3B). These results demonstrate that despite the change in the plasticity gain in 4E-BP-KO mice, synaptic plasticity at PF-PC synapses remains dependent on acute eIF4F formation.

Inhibition of PP2A restores normal LTD in 4E-BP-KO cerebellar slices

Serine/threonine kinase/phosphatase activity downstream of calcium influx plays a critical role in determining whether repeated stimuli will produce LTP as opposed to LTD (Jorntell and Hansel, 2006; Kawaguchi and Hirano, 2013). In response to a large rise in calcium influx, kinase activity gains the upper hand, phosphorylating and internalizing AMPARs, leading to LTD, whereas a small rise in calcium influx shifts the balance toward phosphatase activity, resulting in dephosphorylation, reinsertion, and stabilization of AMPARs, thereby giving rise to LTP. As such, it is conceivable that in cerebella from 4E-BP KO mice, abnormally high phosphatase activity caused LTD stimulation protocols to induce LTP instead of LTD. To test this, we used okadaic acid (1 μM), which inhibits protein phosphatase 1 (PP1) and protein phosphatase 2A (PP2A), two phosphatases that are known to be involved in LTP at PF-PC synapses (Belmeguenai and Hansel, 2005). Previous work showed that phosphatase inhibitors do not block LTD at PF-PC synapses in cerebellar slices from WT mice (Belmeguenai and Hansel, 2005). We observed a robust inhibition of LTP induction in WT slices treated with okadaic acid (86.91% ± 5.99%, t = 26–30 min, n = 4, Figure S3A). Strikingly, after treating cerebellar slices from 4E-BP-KO mice with okadaic acid and stimulating PF with LTD-inducing protocols, EPSCs at PF-PC synapses underwent LTD to ∼85% of baseline (84.01% ± 7.67%, t = 26–30 min, n = 6, Figure 4A), comparable to LTD in WTs (p = 0.77).

Next, we investigated the involvement of each of these phosphatases, as well as protein phosphatase 2B (PP2B), separately using specific inhibitors: PP1 inhibitory peptide inhibitor-2 (I-2) (100 nM), PP2B-selective inhibitor cyclosporin A (100 μm), and PP2A inhibitor fostriecin (50 nM). All three inhibitors blocked LTP induction in cerebellar slices from both WT and 4E-BP-KO (Figures S3B–S3G). Importantly, however, only inhibition of PP2A was effective in restoring LTD in 4E-BP-KO cerebellar slices with LTD-inducing stimuli (Figures 4B–4D). In WT slices, fostriecin (50 nM) or okadaic acid (1 μM) did not affect LTD expression (Figures S3H and S3I). Together, these data indicate that aberrant activity of PP2A, but not PP1 or PP2B, is largely responsible for the conversion of LTD to LTP at PF-PC synapses in 4E-BP-KO cerebellar slices.

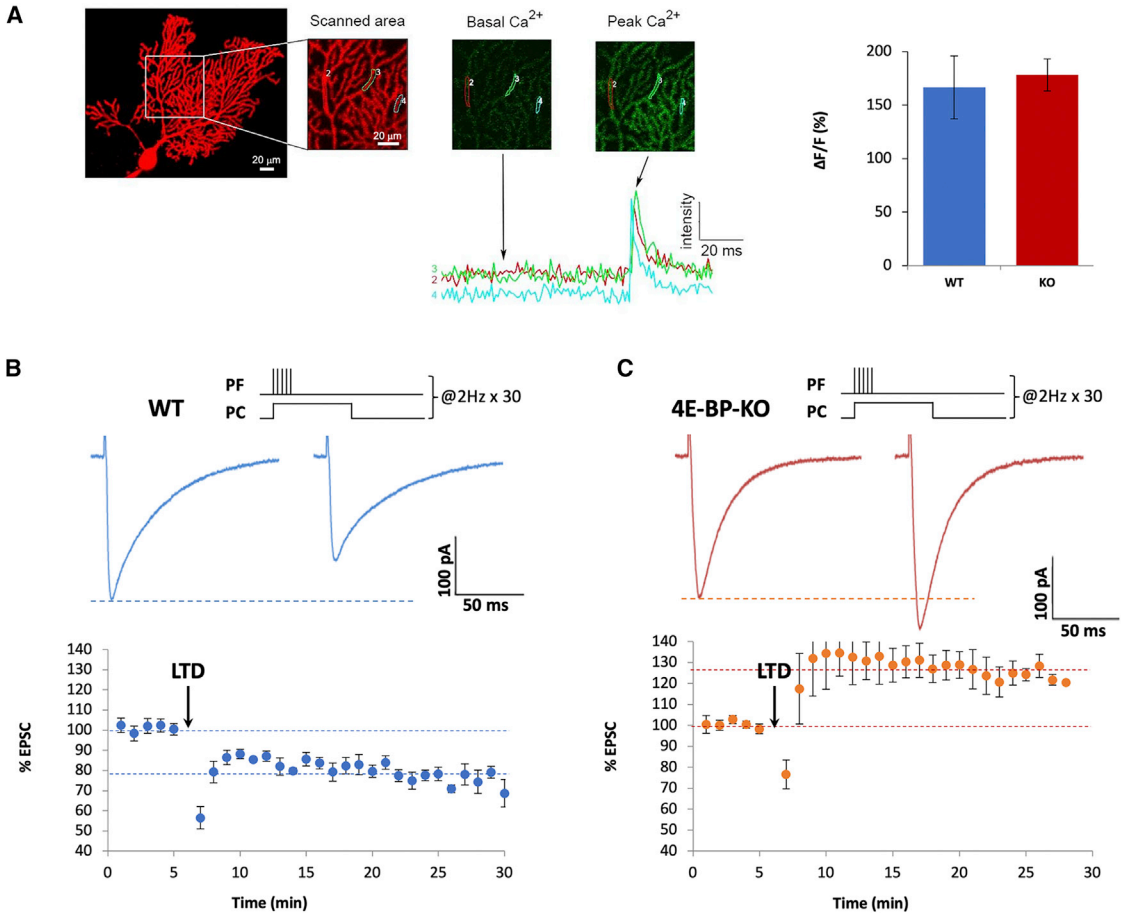

Figure 2. Conversion of PF-PC LTD to LTD in 4E-BP-KO mice is not due to a change in calcium influx and persists using an alternative stimulation protocol

(A) Left to right: representative images of a PC filled with Alexa Fluor 568 (red), the corresponding OGB-1 signal (green), and the change in fluorescent intensity in response to a depolarizing voltage step. Scanned areas were selected using the Alexa Fluor 568 signal; example areas are labeled in the first inset as 2, 3, and 4. Calcium levels were measured in these areas of interest over time by measuring the OGB-1 fluorescent signal. To induce calcium influx, a 100-ms depolarizing voltage step was delivered to the PC cell body through a patch electrode. The bar graph shows normalized average change in fluorescence in WT and 4E-BP-KO cerebellar slices (n = 4).

(B) In WT mice, an alternate LTD protocol consisting of parallel fibers trains of five pulses at 100 Hz accompanied by 100-ms-long depolarization of the Purkinje cell to 0 mV repeated 30 times at 2-s intervals depresses PF-EPSCs (79.05% ± 2.72%, t = 25–30 min, n = 6, paired Student's t test p = 0.00041).

(C) In 4E-BP-KO mice, this protocol potentiates PF-EPSCs (119.442% ± 5.73%, t = 21–25 min, n = 6, paired Student's t test p = 0.0047), significantly different from WTs (Mann-Whitney U test p < 0.00001). All error bars are standard error of the mean.

These experiments raise the possibility that genetic removal of 4E-BP has led to an enhancement of PP2A activity, shifting the balance of kinase/phosphatase in the cerebellum. To test this idea further, we examined protein extracts from WT and 4E-BP-KO cerebellar slices with western blot analysis. PP2A is a multi-protein complex composed of regulatory and catalytic subunits, as well as proteins that influence PP2A activity: the PP2A inhibitor, protein phosphatase methylesterase-1 (PPME1), and the PP2A activator, protein phosphatase 2A phosphatase activator (PTPA) (Kaur and Westermarck, 2016). We did not find any significant differences in the level of expression of PP2A catalytic subunit, Ca/β, structural subunit, Aα/β, or any of the regulatory subunits 55β, 55α, 56ε, or 56δ (Figure 5). Strikingly, we found an average 40% increase in PTPA levels ($p < 0.01$, n= 3) in 4E-BP-deficient cerebella compared with those in WT mice (Figure 5B). The increase in PTPA protein expression is consistent with increased PP2A activity in the cerebella from 4E-BP KO mice. To verify whether PPTA activity is enhanced in 4E-BP mutant mice, we conducted an *in vitro* phosphatase assay using PP2A extracted from wither WT or KO mice. We used *in-vitro*-translated 4E-BP1 as a substrate for PP2A function (Kolupaeva, 2019). We assessed the phosphorylation state of 4E-BP1 at three sites, pS65, pT70, and pT37/T46, following treatment with PP2A-C (catalytic subunit) extracted from either WT or 4E-BP-KO cerebella. This assessment revealed that PP2A-C extracted from 4E-BP-KO mice was significantly more effective than that extracted from WT mice in dephosphorylation of 4E-BP1 (Figure 5B). At higher amounts

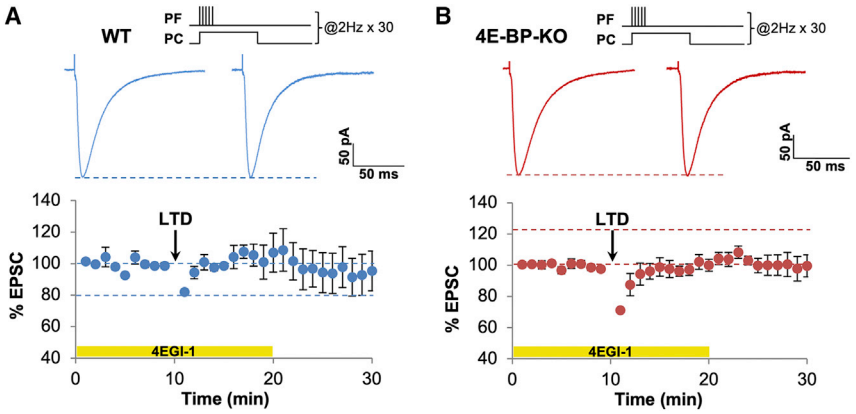

Figure 3. PF-PC LTD in WT and the converted LTP in 4E-BP-KO mice are equally dependent on cap-dependent translation

(A) In WTs, applying 4EGI-1 (50 μM) to cerebellar slices before inducing PF-PC LTD with the burst stimulation and conjunctive depolarization protocol blocks LTD (98.03% ± 5.38%, t = 26–30 min, n = 5, paired Student's t test p = 0.81).

(B) In slices from 4E-BP-KO cerebella, 4EGI-1 prevented the LTD-inducing stimuli from producing a change from baseline (97.73% ± 3.50%, t = 26–30 min, n = 6, paired Student's t test p = 0.37). All error bars are standard error of the mean.

the difference in effectiveness of PP2A-C was more clearly detected at all phosphorylation sites (Figures 5B, 5C, and S4). These results, together with our pharmacological evidence, indicate that the conversion of LTD to LTP at PF-PC synapses in 4E-BP-KO cerebellar slices is associated with an upregulation of PP2A activity. This increase shifts the cellular phosphorylation balance toward net dephosphorylation, thereby altering the plasticity gain from LTD to LTP.

DISCUSSION

We demonstrate that genetic removal of 4E-BP1/2 affects synaptic plasticity in the cerebellum by fundamentally changing the ability of the PF-PC synapses to undergo LTD. Surprisingly, we find that not only do these synapses fail to show depression, but rather they undergo potentiation. We show that this defect could not be attributed to any detectable changes in the cerebellar electrophysiological properties at PF-PC and CF-PC synapses; therefore, it most likely stemmed from a change in the basal phosphatase activity. Many lines of evidence suggest that long-term plasticity at PF-PC synapses in the cerebellar cortex is governed by a tight equilibrium between opposing forces exerted by kinases and phosphatases. Our detailed pharmacological and biochemical interrogation indicates that increased PP2A activity accounts for the striking defect in cerebellar synaptic plasticity in 4E-BP mutant mice. We propose a model in which appropriate kinase activity required for triggering LTD at PF-PC synapses is ensured by the inhibitory action of 4E-BP on phosphatase function. In the absence of 4E-BP, this inhibitory action is removed, which then gives rise to an increase in basal PP2A activity in PCs, rerouting molecular cascades that normally produce LTD to trigger LTP.

The kinase and phosphatase pathways overlap considerably (Kawaguchi and Hirano, 2013), and interestingly, the plasticity curve in 4E-BP mice induced with the LTD protocols shows an induced initial depression followed by a potentiation. These dynamics suggest that initially the kinases act sooner than the phosphatases and dominate the initial response, but at later times, it is the phosphatase pathways that dominate. Interestingly, when applying the LTP protocol to PF-PC synapses in cerebellar slices from 4E-BP KO mice, the magnitude of potentiation was not statistically different than that in WT, presumably because the LTP reaches a maximum.

Loss of 4E-BP-2 leads to an enhancement of both LTP and LTD in the hippocampus (Banko et al., 2005); this enhancement was interpreted to be the result of higher availability of eIF4E and the subsequent increase in protein synthesis (Banko et al., 2005, 2007). Consistent with this interpretation, we found that the translation inhibitor, 4EGI-1, blocked the induction of LTP and LTD at PF-PC synapses in cerebellar slices from 4E-BP-KO mice. Therefore, in spite of the removal of a major regulator of translation, long-term synaptic plasticity remained fundamentally dependent on *de novo* protein synthesis, as shown previously with the general translation inhibitor M7GpppG (Karachot et al., 2001). On the other hand, the loss of 4E-BP did not enhance LTD at PF-PC synapses, but instead converted it to LTP, indicating important differences in regulating synaptic plasticity at hippocampal and cerebellar PF-PC synapses.

The conversion of LTD to LTP at PF-PC synapse in cerebella from 4E-BP-KO mice led us to hypothesize that the loss of 4E-BP altered the balance between kinase and phosphatase activity. It is well accepted that this balance is critical for determining the gain of cerebellar plasticity (Ito, 2002); in particular, increased phosphatase activity promotes the expression of LTP at PF-PC synapses (Belmeguenai and Hansel, 2005). Initial support for our hypothesis came from our pharmacological experiments with the pan phosphatase inhibitor, okadaic acid: okadaic acid prevented the conversion to LTP in 4E-BP cerebella and conjunctive PF stimulation with PC depolarization-induced LTD, as in cerebella from WT mice. Further pharmacological experiments implicate PP2A in PCs as the relevant phosphatase in this conversion of LTD to LTP, while ruling out a direct role for PP2B or PP1. Strong support for PP2A's involvement comes from our biochemical experiments. Our western blot analysis shows that while the expression of regulatory or catalytic subunits of PP2A were unaffected, the expression of the activator of PP2A, a subunit that regulates the activity of PP2A, was increased in 4E-BP-KO cerebella. We further measured an increase in PP2A activity from cerebellar extracts obtained from 4E-BP-KO mice compared with those from WT mice. These findings together provide a mechanistic insight into how 4E-BP normally ensures the integrity of cerebellar synaptic plasticity. While specific phosphatases have been shown to exert cell-autonomous actions on cerebellar plasticity (Schonewille et al., 2010),

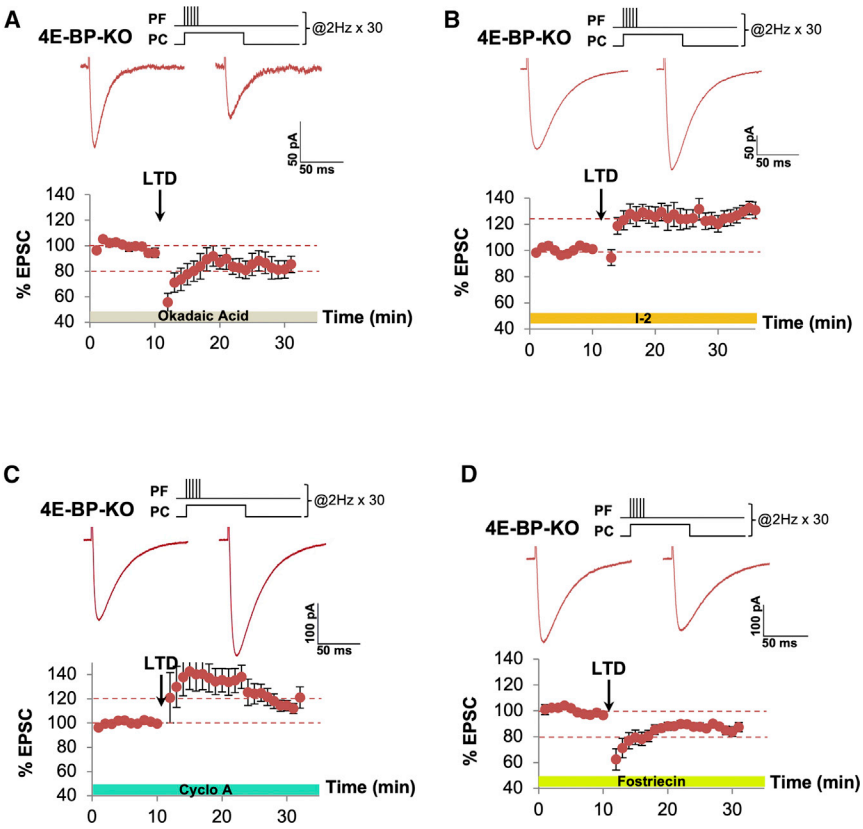

Figure 4. Inhibiting PP2A phosphatase activity in 4E-BP-KO cerebellar slices restores LTD

(A) In 4E-BP-KO cerebellar slices, LTD stimulation in the presence of okadaic acid restores LTD, depressing PF-EPSCs to ~85% of baseline (84.01% ± 7.67%, t = 26–30 min, n = 6, paired Student's t test p = 0.0405), comparable to LTD in WTs (Mann-Whitney U test p = 0.77).

(B) Pharmacological inhibition of PP1 with I-2 (100 nM) has no effect on the potentiation induced with the LTD protocol in 4E-BP-KO mice (124.29% ± 6.14%, t = 26–30 min, n = 9, paired Student's t test p = 0.0044).

(C) Pharmacological inhibition of PP2B with the antagonist cyclosporin A (100 μM) has no effect on the potentiation induced by the LTD protocol (129.55% ± 8.68%, t = 26–30 min, n = 5, paired Student's t test p = 0.025).

(D) Blocking PP2A using the pharmacological inhibitor fostriecin (50 nm) during LTD induction blocks the potentiation and depresses synapses to ~85% of baseline (86.04% ± 2.29%, t = 26–30 min, n = 8, paired Student's t test p = 0.00013), restoring LTD in 4E-BP-KO cerebellar slices. All error bars are standard error of the mean.

it remains to be tested whether the action of PP2A specifically in PCs is critical for the conversion of LTD to LTP in 4E-BP mutant mice.

Our electrophysiological experiments focused on postsynaptic plasticity at PF-PC synapses, but these western blot experiments are not restricted to PCs, and consequently, these changes in PP2A activity likely occur in other cerebellar cell types. And, while our experiments do not directly examine translational regulation of a particular target, we favor the idea that 4E-BP-dependent translational regulation is responsible for setting the basal activity of PP2A and therefore the critical balance between kinases and phosphatases required for normal synaptic plasticity in the cerebellum. Interestingly, we find an enhancement in protein levels of PTPA, only one of the several relevant PP2A protein complexes. It is possible that regulatory features of the 5′-UTR of PP2A mRNA renders it particularly sensitive to the availability of the cap-binding complex for its translation and hence more sensitive to 4E-BP loss of function. Additional experiments are needed to test this idea using both polysome profiling analysis as well as *in vitro* translation assays.

It is particularly interesting that 4E-BP is itself a target of PP2A phosphatase activity (Kolupaeva, 2019) (Nho and Peterson, 2011). Our discovery that 4E-BP negatively regulates PP2A activity points to a potential equilibrium between these two proteins: as 4E-BP is phosphorylated and deactivated, PP2A activity is enhanced, leading to dephosphorylation and activation of 4E-BP. In the absence of 4E-BP, this equilibrium is disrupted and leads to higher PP2A activity. Finally, as the mice used in our study were deficient of 4E-BP1 and 4E-BP2 throughout development, we cannot rule out the possibility that a compensatory change in the state of translational regulation has taken place to balance the loss 4E-BPs (Yanagiya et al., 2012).

Previous work showed that mice with a deletion in the gene for 4E-BP2 have autistic-like behaviors (Gkogkas et al., 2013). Recently, however, it has been reported that selective deletion of the 4E-BP in postnatal mouse PCs resulted in impairment in spatial memory but not in social interaction nor in repetitive behavior (Hooshmandi et al., 2021). In addition, these authors did not detect deficits in LTD at PF-PC synapses, although, given the postnatal expression of the Pcp-2 (L7) promoter used for the condition gene deletion, it is uncertain how much 4E-BP protein had been diminished at the time the synaptic plasticity experiments were conducted compared to the case of constitutive loss of 4E-BP1/4E-BP2 in our study.

Limitations of the study

Our findings suggest that the abnormal enhancement of PP2A activity is responsible for the abnormal expression of LTD at PF-PC synapses in the cerebella of 4E-BP KO mice. In support of this hypothesis, we show that PTPA, an activator of PP2A, is abnormally upregulated in the cerebella of 4E-BP1/2 mice and demonstrate that pharmacological inhibition of PP2A restores normal LTD in 4E-BP1/2 mice. In spite of these findings, our dataset does not provide sufficient evidence that either 4E-BP or PP2A function cell autonomously in PCs. In addition, while we favor the idea that PTPA is under the translational control of 4E-BP, our dataset does not directly verify this relationship. It

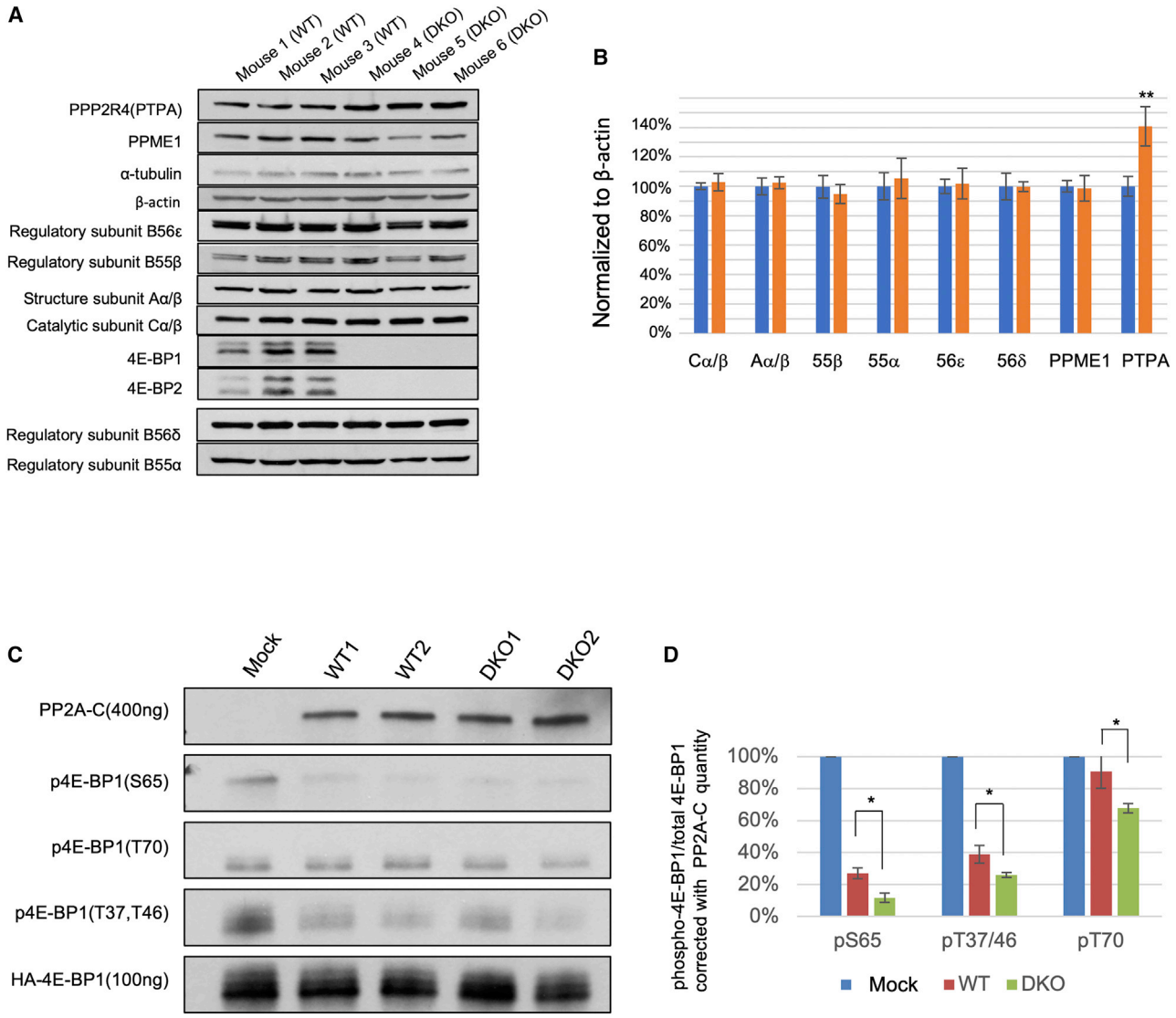

Figure 5. PP2A activity is increased in 4E-BP-KO cerebella likely due to an increase in the expression of PP2A regulator PPTA

(A) Western blot of 4E-BP1/2-KO and WT cerebella, staining for PP2A subunits and its regulators. Regulatory subunit B56δ and B56α are from the same samples but ran on another membrane. Please also see Figure S5 for additional western blots.

(B) Quantification of signals in (A). Three mice were used per genotype; the western analysis was repeated three times similarly to (A), and all three were included in our quantification. **$p < 0.01$.

(C) Western blot of 4E-BP1/2-KO and WT cerebella, staining for PP2A extracted from corresponding cerebella, and 4E-BP1 protein generated from HEK293 cells. Decrease in phosphorylation states of 4E-BP1, as a known substrate of PP2A, were used as an indication of PP2A phosphatase activity.

(D) Quantification of signals in (C). pS65 antibody recognizes the upper band of 4E-BP1 gel isoforms. pT70 antibody recognizes the lowest two bands of 4E-BP1 gel isoforms. pT37/T46 antibody recognizes all gel isoforms of 4E-BP1. All error bars are standard error of the mean.

is likely that another intermediate translational target of 4E-BP is responsible for the stability of PTPA protein.

STAR★METHODS

Detailed methods are provided in the online version of this paper and include the following:

- KEY RESOURCES TABLE
- RESOURCE AVAILABILITY
  - Lead contact
  - Materials availability
  - Data and code availability
- EXPERIMENTAL MODEL AND SUBJECT DETAILS
  - Mice
- METHOD DETAILS
  - Cerebellar slice preparation
  - Electrophysiological recordings in the cerebellum

- LTD protocols
- LTP protocol
- Pharmacological inhibitors
- Calcium imaging
- Western blot analysis
- Phosphatase assay
- Calbindin staining in the cerebellum

- QUANTIFICATION AND STATISTICAL ANALYSIS

SUPPLEMENTAL INFORMATION

Supplemental information can be found online at https://doi.org/10.1016/j.celrep.2022.110911.

ACKNOWLEDGMENTS

Supported by Canadian Institute of Health Research operating grants to A.P.H., E.C., D.B., and N.S. Additional funding was provided to A.P.H. by operating funds at the Buck Institute for Aging Research.

AUTHOR CONTRIBUTIONS

Conceptualization, N.S., E.C., and A.P.H.; methodology, N.S., E.C., Y.C., and A.P.H.; investigation, N.S., Y.C., P.W., S.B., Z.Z., and A.A.B.; writing – original draft, N.S., A.P.H., and E.C.; writing – review & editing, N.S., A.P.H., E.C., P.W., and N.S.; visualization, N.S., E.C., and A.P.H.; funding acquisition, A.P.H., E.C., D.B., and N.S.

DECLARATION OF INTERESTS

The authors have no financial interests or conflicts of interest.

Received: March 16, 2021
Revised: October 31, 2021
Accepted: May 12, 2022
Published: June 7, 2022

REFERENCES

Adams, D.G., and Wadzinski, B.E. (2007). Isolation and characterization of PP2A holoenzymes containing FLAG-tagged B subunits. Methods Mol. Biol. *365*, 101–111. https://doi.org/10.1385/1-59745-267-x:101.

Aguilar-Valles, A., Matta-Camacho, E., Khoutorsky, A., Gkogkas, C., Nader, K., Lacaille, J.C., and Sonenberg, N. (2015). Inhibition of group I metabotropic glutamate receptors reverses autistic-like phenotypes caused by deficiency of the translation repressor eIF4E binding protein 2. J. Neurosci. *35*, 11125–11132. https://doi.org/10.1523/jneurosci.4615-14.2015.

Alba, A., Kano, M., Chen, C., Stanton, M.E., Fox, G.D., Herrup, K., Zwingman, T.A., and Tonegawa, S. (1994). Deficient cerebellar long-term depression and impaired motor learning in mGluR1 mutant mice. Cell *79*, 377–388. https://doi.org/10.1016/0092-8674(94)90205-4.

Banko, J.L., Poulin, F., Hou, L., DeMaria, C.T., Sonenberg, N., and Klann, E. (2005). The translation repressor 4E-BP2 is critical for eIF4F complex formation, synaptic plasticity, and memory in the hippocampus. J. Neurosci. *25*, 9581–9590. https://doi.org/10.1523/jneurosci.2423-05.2005.

Banko, J.L., Merhav, M., Stern, E., Sonenberg, N., Rosenblum, K., and Klann, E. (2007). Behavioral alterations in mice lacking the translation repressor 4E-BP2. Neurobiol. Learn. Mem. *87*, 248–256. https://doi.org/10.1016/j.nlm.2006.08.012.

Belmeguenai, A., and Hansel, C. (2005). A role for protein phosphatases 1, 2A, and 2B in cerebellar long-term potentiation. J. Neurosci. *25*, 10768–10772. https://doi.org/10.1523/jneurosci.2876-05.2005.

Bidinosti, M., Ran, I., Sanchez-Carbente, M.R., Martineau, Y., Gingras, A.C., Gkogkas, C., Raught, B., Bramham, C.R., Sossin, W.S., Costa-Mattioli, M., et al. (2010). Postnatal deamidation of 4E-BP2 in brain enhances its association with raptor and alters kinetics of excitatory synaptic transmission. Mol. Cell *37*, 797–808. https://doi.org/10.1016/j.molcel.2010.02.022.

Chong, Y., Saviuk, N., Pie, B., Basisty, N., Quinn, R.K., Schilling, B., Sonenberg, N., Cooper, E., and Haghighi, A.P. (2018). Removing 4E-BP enables synapses to refine without postsynaptic activity. Cell Rep. *23*, 11–22. https://doi.org/10.1016/j.celrep.2018.03.040.

Coesmans, M., Weber, J.T., De Zeeuw, C.I., and Hansel, C. (2004). Bidirectional parallel fiber plasticity in the cerebellum under climbing fiber control. Neuron *44*, 691–700. https://doi.org/10.1016/j.neuron.2004.10.031.

Cupolillo, D., Hoxha, E., Faralli, A., De Luca, A., Rossi, F., Tempia, F., and Carulli, D. (2016). Autistic-like traits and cerebellar dysfunction in Purkinje cell PTEN knock-out mice. Neuropsychopharmacology *41*, 1457–1466. https://doi.org/10.1038/npp.2015.339.

De Zeeuw, C.I., Hansel, C., Bian, F., Koekkoek, S.K., van Alphen, A.M., Linden, D.J., and Oberdick, J. (1998). Expression of a protein kinase C inhibitor in Purkinje cells blocks cerebellar LTD and adaptation of the vestibulo-ocular reflex. Neuron *20*, 495–508. https://doi.org/10.1016/s0896-6273(00)80990-3.

Feil, R., Hartmann, J., Luo, C., Wolfsgruber, W., Schilling, K., Feil, S., Barski, J.J., Meyer, M., Konnerth, A., De Zeeuw, C.I., and Hofmann, F. (2003). Impairment of LTD and cerebellar learning by Purkinje cell-specific ablation of cGMP-dependent protein kinase I. J. Cell Biol. *163*, 295–302. https://doi.org/10.1083/jcb.200306148.

Gingras, A.C., Gygi, S.P., Raught, B., Polakiewicz, R.D., Abraham, R.T., Hoekstra, M.F., Aebersold, R., and Sonenberg, N. (1999). Regulation of 4E-BP1 phosphorylation: a novel two-step mechanism. Genes Dev. *13*, 1422–1437. https://doi.org/10.1101/gad.13.11.1422.

Gkogkas, C.G., Khoutorsky, A., Ran, I., Rampakakis, E., Nevarko, T., Weatherill, D.B., Vasuta, C., Yee, S., Truitt, M., Dallaire, P., et al. (2013). Autism-related deficits via dysregulated eIF4E-dependent translational control. Nature *493*, 371–377. https://doi.org/10.1038/nature11628.

Haghighat, A., Mader, S., Pause, A., and Sonenberg, N. (1995). Repression of cap-dependent translation by 4E-binding protein 1: competition with p220 for binding to eukaryotic initiation factor-4E. EMBO J. *14*, 5701–5709. https://doi.org/10.1002/j.1460-2075.1995.tb00257.x.

Hansel, C., de Jeu, M., Belmeguenai, A., Houtman, S.H., Buitendijk, G.H., Andreev, D., De Zeeuw, C.I., and Elgersma, Y. (2006). αCaMKII is essential for cerebellar LTD and motor learning. Neuron *51*, 835–843. https://doi.org/10.1016/j.neuron.2006.08.013.

Hooshmandi, M., Truong, V.T., Fields, E., Thomas, R.E., Wong, C., Sharma, V., Gantois, I., Soriano Roque, P., Chalkiadaki, K., Wu, N., et al. (2021). 4E-BP2-dependent translation in cerebellar Purkinje cells controls spatial memory but not autism-like behaviors. Cell Rep *35*, 109036.

Ito, M. (2002). The molecular organization of cerebellar long-term depression. Nat. Rev. Neurosci. *3*, 896–902. https://doi.org/10.1038/nrn962.

Jorntell, H., and Hansel, C. (2006). Synaptic memories upside down: bidirectional plasticity at cerebellar parallel fiber-Purkinje cell synapses. Neuron *52*, 227–238. https://doi.org/10.1016/j.neuron.2006.10.015.

Kakegawa, W., Miyazaki, T., Emi, K., Matsuda, K., Kohda, K., Motohashi, J., Mishina, M., Kawahara, S., Watanabe, M., and Yuzaki, M. (2008). Differential regulation of synaptic plasticity and cerebellar motor learning by the C-terminal PDZ-binding motif of GluR 2. J. Neurosci. *28*, 1460–1468. https://doi.org/10.1523/jneurosci.2553-07.2008.

Kakegawa, W., and Yuzaki, M. (2005). A mechanism underlying AMPA receptor trafficking during cerebellar long-term potentiation. Proc. Natl. Acad. Sci. U S A *102*, 17846–17851. https://doi.org/10.1073/pnas.0508910102.

Karachot, L., Shirai, Y., Vigot, R., Yamamori, T., and Ito, M. (2001). Induction of long-term depression in cerebellar Purkinje cells requires a rapidly turned over protein. J. Neurophysiol. *86*, 280–289. https://doi.org/10.1152/jn.2001.86.1.280.

Kashiwabuchi, N., Ikeda, K., Araki, K., Hirano, T., Shibuki, K., Takayama, C., Inoue, Y., Kutsuwada, T., Yagi, T., Kang, Y., et al. (1995). Impairment of motor coordination, Purkinje cell synapse formation, and cerebellar long-term

depression in GluR delta 2 mutant mice. Cell *81*, 245–252. https://doi.org/10.1016/0092-8674(95)90334-8.

Kaur, A., and Westermarck, J. (2016). Regulation of protein phosphatase 2A (PP2A) tumor suppressor function by PME-1. Biochem. Soc. Trans. *44*, 1683–1693. https://doi.org/10.1042/bst20160161.

Kawaguchi, S.Y., and Hirano, T. (2013). Gating of long-term depression by Ca2+/calmodulin-dependent protein kinase II through enhanced cGMP signalling in cerebellar Purkinje cells. J. Physiol. *591*, 1707–1730. https://doi.org/10.1113/jphysiol.2012.245787.

Kloth, A.D., Badura, A., Li, A., Cherskov, A., Connolly, S.G., Giovannucci, A., Bangash, M.A., Grasselli, G., Penagarikano, O., Piochon, C., et al. (2015). Cerebellar associative sensory learning defects in five mouse autism models. Elife *4*, e06085. https://doi.org/10.7554/elife.06085.

Kolupaeva, V. (2019). Serine-threonine protein phosphatases: lost in translation. Biochim. Biophys. Acta Mol. Cell Res. *1866*, 83–89. https://doi.org/10.1016/j.bbamcr.2018.08.006.

Leitges, M., Kovac, J., Plomann, M., and Linden, D.J. (2004). A unique PDZ ligand in PKCα confers induction of cerebellar long-term synaptic depression. Neuron *44*, 585–594. https://doi.org/10.1016/j.neuron.2004.10.024.

Lev-Ram, V., Wong, S.T., Storm, D.R., and Tsien, R.Y. (2002). A new form of cerebellar long-term potentiation is postsynaptic and depends on nitric oxide but not cAMP. Proc. Natl. Acad. Sci. U S A *99*, 8389–8393. https://doi.org/10.1073/pnas.122206399.

Linden, D.J. (1996). A protein synthesis-dependent late phase of cerebellar long-term depression. Neuron *17*, 483–490. https://doi.org/10.1016/s0896-6273(00)80180-4.

Linden, D.J., and Connor, J.A. (1991). Participation of postsynaptic PKC in cerebellar long-term depression in culture. Science *254*, 1656–1659. https://doi.org/10.1126/science.1721243.

Mader, S., Lee, H., Pause, A., and Sonenberg, N. (1995). The translation initiation factor eIF-4E binds to a common motif shared by the translation factor eIF-4 gamma and the translational repressors 4E-binding proteins. Mol. Cell Biol. *15*, 4990–4997. https://doi.org/10.1128/mcb.15.9.4990.

Marcotrigiano, J., Gingras, A.C., Sonenberg, N., and Burley, S.K. (1999). Cap-dependent translation initiation in eukaryotes is regulated by a molecular mimic of eIF4G. Mol. Cell *3*, 707–716. https://doi.org/10.1016/s1097-2765(01)80003-4.

Miyata, M., Kim, H.T., Hashimoto, K., Lee, T.K., Cho, S.Y., Jiang, H., Wu, Y., Jun, K., Wu, D., Kano, M., and Shin, H.S. (2001). Deficient long-term synaptic depression in the rostral cerebellum correlated with impaired motor learning in phospholipase C β4 mutant mice. Eur. J. Neurosci. *13*, 1945–1954. https://doi.org/10.1046/j.0953-816x.2001.01570.x.

Nho, R.S., and Peterson, M. (2011). Eukaryotic translation initiation factor 4E binding protein 1 (4EBP-1) function is suppressed by Src and protein phosphatase 2A (PP2A) on extracellular matrix. J. Biol. Chem. *286*, 31953–31965. https://doi.org/10.1074/jbc.m111.222299.

Pause, A., Belsham, G.J., Gingras, A.C., Donze, O., Lin, T.A., Lawrence, J.C., Jr., and Sonenberg, N. (1994). Insulin-dependent stimulation of protein synthesis by phosphorylation of a regulator of 5'-cap function. Nature *371*, 762–767. https://doi.org/10.1038/371762a0.

Ran, I., Laplante, I., Bourgeois, C., Pepin, J., Lacaille, P., Costa-Mattioli, M., Pelletier, J., Sonenberg, N., and Lacaille, J.C. (2009). Persistent transcription- and translation-dependent long-term potentiation induced by mGluR1 in hippocampal interneurons. J. Neurosci. *29*, 5605–5615. https://doi.org/10.1523/jneurosci.5355-08.2009.

Ran, I., Gkogkas, C.G., Vasuta, C., Tartas, M., Khoutorsky, A., Laplante, I., Parsyan, A., Nevarko, T., Sonenberg, N., and Lacaille, J.C. (2013). Selective regulation of GluA subunit synthesis and AMPA receptor-mediated synaptic function and plasticity by the translation repressor 4E-BP2 in hippocampal pyramidal cells. J. Neurosci. *33*, 1872–1886. https://doi.org/10.1523/jneurosci.3264-12.2013.

Richter, J.D., and Sonenberg, N. (2005). Regulation of cap-dependent translation by eIF4E inhibitory proteins. Nature *433*, 477–480. https://doi.org/10.1038/nature03205.

Schonewille, M., Belmeguenai, A., Koekkoek, S.K., Houtman, S.H., Boele, H.J., van Beugen, B.J., Gao, Z., Badura, A., Ohtsuki, G., Amerika, W.E., et al. (2010). Purkinje cell-specific knockout of the protein phosphatase PP2B impairs potentiation and cerebellar motor learning. Neuron *67*, 618–628. https://doi.org/10.1016/j.neuron.2010.07.009.

Shin, J.H., and Linden, D.J. (2005). An NMDA receptor/nitric oxide cascade is involved in cerebellar LTD but is not localized to the parallel fiber terminal. J. Neurophysiol. *94*, 4281–4289. https://doi.org/10.1152/jn.00661.2005.

Sonenberg, N., and Hinnebusch, A.G. (2009). Regulation of translation initiation in eukaryotes: mechanisms and biological targets. Cell *136*, 731–745. https://doi.org/10.1016/j.cell.2009.01.042.

Sonenberg, N., Rupprecht, K.M., Hecht, S.M., and Shatkin, A.J. (1979). Eukaryotic mRNA cap binding protein: purification by affinity chromatography on sepharose-coupled m7GDP. Proc. Natl. Acad. Sci. U S A *76*, 4345–4349. https://doi.org/10.1073/pnas.76.9.4345.

Ting, J.T., Daigle, T.L., Chen, Q., and Feng, G. (2014). Acute brain slice methods for adult and aging animals: application of targeted patch clamp analysis and optogenetics. Methods Mol. Biol. *1183*, 221–242. https://doi.org/10.1007/978-1-4939-1096-0_14.

Tsai, P.T., Hull, C., Chu, Y., Greene-Colozzi, E., Sadowski, A.R., Leech, J.M., Steinberg, J., Crawley, J.N., Regehr, W.G., and Sahin, M. (2012). Autistic-like behaviour and cerebellar dysfunction in Purkinje cell Tsc1 mutant mice. Nature *488*, 647–651. https://doi.org/10.1038/nature11310.

Tsukiyama-Kohara, K., Poulin, F., Kohara, M., DeMaria, C.T., Cheng, A., Wu, Z., Gingras, A.C., Katsume, A., Elchebly, M., Spiegelman, B.M., et al. (2001). Adipose tissue reduction in mice lacking the translational inhibitor 4E-BP1. Nat. Med. *7*, 1128–1132. https://doi.org/10.1038/nm1001-1128.

Uemura, T., Kakizawa, S., Yamasaki, M., Sakimura, K., Watanabe, M., Iino, M., and Mishina, M. (2007). Regulation of long-term depression and climbing fiber territory by glutamate receptor 2 at parallel fiber synapses through its C-terminal domain in cerebellar Purkinje cells. J. Neurosci. *27*, 12096–12108. https://doi.org/10.1523/jneurosci.2680-07.2007.

van Woerden, G.M., Hoebeek, F.E., Gao, Z., Nagaraja, R.Y., Hoogenraad, C.C., Kushner, S.A., Hansel, C., De Zeeuw, C.I., and Elgersma, Y. (2009). βCaMKII controls the direction of plasticity at parallel fiber–Purkinje cell synapses. Nat. Neurosci. *12*, 823–825. https://doi.org/10.1038/nn.2329.

Yanagiya, A., Suyama, E., Adachi, H., Svitkin, Y.V., Aza-Blanc, P., Imataka, H., Mikami, S., Martineau, Y., Ronai, Z.A., and Sonenberg, N. (2012). Translational homeostasis via the mRNA cap-binding protein, eIF4E. Mol Cell *46*, 847–858.

Yuzaki, M. (2013). Cerebellar LTD vs. motor learning-lessons learned from studying GluD2. Neural Netw. *47*, 36–41. https://doi.org/10.1016/j.neunet.2012.07.001.

STAR★METHODS

KEY RESOURCES TABLE

REAGENT or RESOURCE	SOURCE	IDENTIFIER
Antibodies		
PPP2R4 (PTPA)	Cell Signaling	#3330; RRID: AB_2170264
PPME1	Bethyl Laboratories	A304-762A; RRID: AB_2620957
regulatory subunit B56ε	Millipore	MABS270
Regulatory subunit B55β	Bettyl Laboratories	A300-964A; RRID: AB_2169968
Structure subunit Aα/β	Cell Signaling	#2039; RRID: AB_490763
Catalytic subunit Cα/β	Santa Cruz	SC-80665; RRID: AB_1128770
4E-BP1	Cell Signaling	#9644; RRID: AB_2097841
4E-BP2	Cell Signaling	#2845; RRID: AB_10699019)
Regulatory subunit B56δ	ThermoFisher	A301-100A; RRID: AB_2168123
Regulatory subunit B55α	ThermoFisher	MA5-15007; RRID: AB_10978041
Monoclonal anti Calbindin D-28k	Swant	C9638;RRID: AB_2314070
Alexa 488-conjugated anti-mouse	Jackson Immunoresearch	code: 115-545-205; RRID: AB_2338854
Chemicals, peptides, and recombinant proteins		
Bicuculline	Tocris	Cat# 0130; CAS: 485-49-4
4EGI-1	Sigma-Aldrich	Cat# 324517; CAS: 315706-13-9
Okadaic Acid, Ammonium Salt	Sigma-Aldrich	Cat# 459616; CAS: 155716-06-6
inhibitory peptide inhibitor-2 (I-2)	New England BioLabs	NEB #P0754
Cyclosporin A	Tocris	Cat# 1101; CAS: 59865-13-3
Fostriecin	Sigma-Aldrich	F4425; CAS: 87860-39-7
Oregon Green BAPTA-1 hexapotassium salt	Invitrogen	O6806
Alexa Fluor 568 hydrazide	Invitrogen	A10437
Experimental models: Organisms/strains		
Mouse: C57BL/6 Eif4ebp1; Eif4ebp2 DKO	Gift from Dr. N. Sonenberg	N/A

RESOURCE AVAILABILITY

Lead contact

Further information and requests for resources and reagents should be directed to and will be fulfilled by the Lead Contact, Pejmun Haghighi (PHaghighi@buckinstitute.org).

Materials availability

This study did not generate new unique reagents.

Data and code availability

- Upon request, any data reported in this paper will be shared by the lead contact.
- This paper does not report original code.
- Any additional information required to reanalyze the data reported in this paper is available from the lead contact upon request.

EXPERIMENTAL MODEL AND SUBJECT DETAILS

Mice

A colony of C57BL/6 Eif4ebp1; Eif4ebp2 DKO mice (gift from Dr. N. Sonenberg) were maintained by breeding homozygous animals (Banko et al., 2005; Tsukiyama-Kohara et al., 2001). Double 4E-BP1/BP2 KO mice on a C57BL/6 background breed normally. Therefore, for our experiments we used progenies from these matings, and progenies from age-matched wild-type C57BL/6 mice, housed in the same colony, as controls. The genotype of mice used for electrophysiological experiments were known to the investigator prior to the experiment.

All mice were maintained under pathogen-free conditions, and cages were maintained in ventilated racks in temperature (20–21°C) and humidity (~55%) controlled rooms on a 12 h light/dark cycle. Standard bedding was used for housing with the addition of Enviro-Dri (Shepherd Specialty Paper). Food and water were provided *ad libitum*. Pups were kept with their dams until weaning. After weaning, mice were group housed (maximum of 6 per cage) by sex. All experiments involved mice 18–25 days old of both sexes.

All procedures were in compliance with the Canadian Council on Animal Care guidelines and were approved by McGill University Animal Care Committees.

METHOD DETAILS

Cerebellar slice preparation

Mice were sacrificed with CO_2 and trans-cardially perfused with 20mL of ice-cold (0°C) HEPES ACSF solution containing (in mM): 92 NaCl, 2.5 KCl, 1.2 NaH_2PO_4, 30 $NaHCO_3$, 20 HEPES, 25 glucose, 5 sodium ascorbate, 2 thiourea, 3 sodium pyruvate, 10 $MgSO_4$, 0.5$CaCl_2$ adjusted to pH 7.4 with NaOH or HCl, and bubbled for at least 30 min prior to use with 95% O_2/5% CO_2. The cerebella were dissected out into HEPES ACSF (0°C), glued to the vibratome cutting platform (Compresstome VF-200, Precisionary Instruments) with cyanoacrylate adhesive and embedded in 2% agar (Sigma). Sagittal slices (250 μm thick) were cut from the cerebellum vermis using a zirconium ceramic blade (EF-INZ10, Cadence) and transferred for recovery into oxygenated standard ACSF consisting of (in mM): 124 NaCl, 2.5 KCl, 1.2 NaH2PO4, 24 NaHCO3, 5 HEPES, 12.5 glucose, 2MgSO4, 2CaCl2 (pH adjusted to 7.4 with NaOH or HCl) until required for recording. All solutions were oxygenated for at least 30 min prior to use (Ting et al., 2014).

For WT LTD recordings quantified in Figures S3H and S3I a few modifications were made: P21-P25 mice were sacrificed by decapitation. Then the cerebellum was extracted within 1 min and submerged into the cutting solution (0°C) consisting of (in mM): 2.5 KCl, 1.25 NaH2PO4, 28 $NaHCO_3$, 0.5 $CaCl_2$, 7 $MgCl_2$, 7 D-glucose, 1 ascorbic acid, 3 sodium pyruvate, 233.7 sucrose for later slicing. The cerebella were glued to the vibratome cutting platform (Compresstome VF-200, Precisionary Instruments) with superglue. Sagittal slices (300 μm thick) were cut from the cerebellum vermis using a zirconium ceramic blade (EF-INZ10, Cadence) and transferred for recovery into oxygenated standard ACSF consisting of (in mM): 125 NaCl, 2.5 KCl, 1.25 NaH_2PO_4, 26 $NaHCO_3$, 25 glucose, 2 $CaCl_2$, 1 $MgCl_2$ until required for recording. 95% O_2/5% CO_2 was bubbled all the time during the slicing.

Electrophysiological recordings in the cerebellum

Whole-cell recordings were obtained from visually identified PCs under a confocal microscope (FV-1000, Olympus) using a 40× water-immersion objective and IR900nm DIC optics. To patch PCs, 2.5–4 MΩ glass electrodes were used, filled with intracellular solution containing (in mM): 60 CsCl, 40 Cs D-gluconate, 20 TEA-Cl, 1 EGTA, 4 $MgCl_2$, 4 ATP, 0.4 GTP, and 30 HEPES, adjusted to pH 7.3 with CsOH. In the recording chamber, the slice was perfused with standard ACSF (4 mL min-1) at room temperature. Bicuculline (10 μM, Tocris) was always added to block IPSPs. To stimulate PFs and CFs, a glass electrode (3–6 μm tip diameter) filled with standard ACSF was used. Focal stimulation of PFs was achieved by applying a square pulses (0.1ms in duration, 100V in amplitude) using a stimulator (World Precision Instruments) in the molecular layer one-third from the pial surface and focal stimulation of CFs was achieved by applying a square pulses (0.1ms in duration, 100V in amplitude) in the granule layer. Ionic currents from PCs were recorded with a VE-2 amplifier (Alembic Software, Montreal, QC, Canada). Series resistance was compensated for (~40–60%), and changes in series resistance and input resistance were monitored by delivering a 50ms long, −5 mV hyperpolarizing voltage step. If series resistance or input resistance changed more than 20%, data was discarded. Stimulation and acquisition were performed with IGOR Pro (WaveMetrics, Lake Oswego, OR), and the data were analyzed offline. The signals were filtered at 3 Hz and digitized at 20 kHz. PF-EPSCs were recorded at a holding potential of −80 mV, and CF-EPSCs at a holding potential of −20 mV. Paired pulse to CFs and PFs were delivered at a 50ms interval. The intrinsic firing frequency of PCs was recorded in a cell-attached configuration.

LTD protocols

LTD was induced using one of two stimulation protocols. The first, by conjunctive stimulation (CJS) (PF stimuli concomitant with 30 ms depolarization of the PC to −30 mV at 1Hz, 300s) after the acquisition of a stable baseline response for 20 min at 0.1 Hz (Uemura et al., 2007). Following the CJS, we recorded the PF-EPSC at a rate of 0.1 Hz for up to 40 min. The amplitude of the baseline PF-EPSCs and the PF-EPSCs following CJS were averaged every 60 s, and the PF-EPSCs following CJS were normalized to the baseline PF-EPSCs for each PC.

The second LTD inducing protocol consists of parallel fibers trains of five pulses at 100 Hz accompanied by 100-ms-long depolarization of the Purkinje cell to 0 mV repeated 30 times at 2-s intervals (Shin and Linden, 2005).

LTP protocol

LTP was induced by stimulating PFs at 1Hz for 300s after the acquisition of a stable baseline response for 20 min at 0.1 Hz. Following the stimulation, we recorded the PF-EPSC at a rate of 0.1 Hz for up to 40 min (Lev-Ram et al., 2002).

Pharmacological inhibitors

To assess the role of individual molecules in the LTD and/or LTP pathway, specific pharmacological inhibitors were either perfused in the extracellular solution or included in the pipette saline.

To block cap-dependent translation initiation during LTD induction, the translation inhibitor 4EGI-1 (50 μm, Calbiochem), which selectively blocks the eIF4E-eIF4G interaction, was perfused in the recording chamber 10 min prior to starting the LTD stimulation until 10 min after the LTD stimulation ended (Gkogkas et al., 2013).

Several pharmacological inhibitors were used to understand the molecular mechanisms involved in PF-PC LTD in the cerebellum on 4E-BP-KOs. To block phosphatase activity in cerebellar slices, the general phosphatase inhibitor Okadaic Acid (1uM, Sigma, St. Louis, MO) was added to the extracellular solution and perfused into the recording chamber 30 min prior to inducing LTD until the end of the recording. To block PP1, inhibitory peptide inhibitor-2 (I-2; 100 nM, New England BioLabs, Beverly, MA) was added to the pipette solution and allowed to perfuse into the PC for 20 min after whole-cell configuration was achieved before recording was started. PP2B was blocked using Cyclosporin A (100uM, Tocris, Ellisville, MO) added to the extracellular solution and perfused into the recording chamber 30 min prior to inducing LTD until the end of the recording. PP2A was inhibited using Fostriecin (50 nm; Sigma, St. Louis, MO) added to the pipette saline (Belmeguenai and Hansel, 2005).

Calcium imaging

Calcium imaging of Purkinje cells was performed on an upright confocal microscope. The intracellular solution contained (in mM) 135 Cs-methanesulfonate, 10 CsCl, 10 HEPES, 4 Na_2ATP, 0.4 Na_3GTP, and 0.15 Oregon Green BAPTA-1 hexapotassium salt (Invitrogen, Carlsbad, CA) and 0.1 Alexa Fluor 568 (Invitrogen, Carlsbad, CA) (pH 7.25). We started imaging 20 min after the establishment of whole-cell configuration to allow for dendritic perfusion of the intracellular solution. Using the Alexa Fluor 568 signal, a region of interest approximately half-way between the cell body and the pial surface was selected. Using a 488 laser, the region of interest was sampled at 10Hz while we delivered a depolarizing voltage step to 0mV for 100ms to the PC cell body at 1Hz. The data was acquired with FluoView and the image data were analyzed with ImageJ.

Western blot analysis

For the cerebellum, mice were sacrificed using CO2, transcardially perfused with standard aCSF, and the cerebella rapidly removed and flash-frozen in liquid nitrogen. Western blot analysis was performed according to manufacturer's protocols using the following primary antibodies against: PPP2B4 (PTPA), PPME1, regulatory subunit B56ε, Regulatory subunit B55β, Structure subunit Aα/β, Catalytic subunit Cα/β, 4E-BP1, 4E-BP2, Regulatory subunit B56δ, Regulatory subunit B55α.

Protein bands were visualized using SuperSignal West Pico Chemiluminescent Substrate (Thermo Scientific). The gel images were scanned, and band intensities were quantified using Image Lab 6.1(Bio-Rad).

Phosphatase assay

Cerebella from WT or DKO mouse were crushed in RIPA buffer and incubated at 4ºC on wheel for 10 min. After 10mins centrifugation at 15000rpm, the supernatant (cerebella lysate) containing 2mg total protein was transferred into a new Eppendorf tube. 2ug PP2A-C antibody (Santa Cruz sc-80665) was added, then the sample was incubated at 4ºC on wheel overnight. The next day, 50ul pre-washed protein G agarose (Millipore 16–266) was added into the tube following incubation at 4ºC on wheel for 1 h. After 2 min centrifugation at 2000 rpm at 4ºC, the supernatant was removed and fresh RIPA buffer was added for washing. After 3 washes, purified PP2A-C on protein G agarose was resuspended in 60ul phosphatase buffer described by Deanna G. Adams and Brian E. Wadzinski (Adams and Wadzinski, 2007) and kept at −80ºC. In addition, HA-4E-BP1 was expressed in HEK293H cells and purified with Anti-HA magnetic beads (Pierce™ 88836), then eluted with HA synthetic peptide (Sino Biological PP100028). 100ng HA-4E-BP1 was mixed with 200–400ng PP2Ac in the phosphatase buffer with final volume 50ul. Then the sample was maintained at 30ºC, 1000rpm for 30mins in Eppendorf thermomixer. The reaction was stopped by adding laemmlie buffer. 10ul of each reaction was loaded on SDS-PAGE gel for WB analysis.

Calbindin staining in the cerebellum

For calbindin immunostaining, mice (P21-P30) were deeply anesthetized by CO_2, cervically dislocated and intracardially perfused with ice-cold HEPES ACSF followed by 4% paraformaldehyde. Brains were postfixed for 2–16 h and equilibrated with 30% sucrose overnight. Sagittal sections (50 μm) were permeabilized in PBS with Triton X-0.25% (Tx-PBS) and treated as follows in Tx-PBS based solutions: they were preincubated with 10% normal donkey serum solution (Jackson Immunoresearch USA, West Grove, PA, USA) for 1 h at room temperature (RT) and incubated with mouse anti-Cb (1:1,000; Swant, Marly, Switzerland; code 300) overnight at 4°C, then incubated with secondary antibody (Alexa 488-conjugated anti-mouse, 1:200; Jackson Immunoresearch) for 2 h at room temperature and rinsed.

For the quantification of Purkinje cell density, images were acquired with a confocal microscope (FV-1000, Olympus) with a 60X, NA 1.42 PlanApo N oil-immersion objective. The data was acquired with FluoView and the image data was analyzed with ImageJ. Calbindin-positive Purkinje cells were counted in random fields (5–10/animal), and their number was normalized by the length of the Purkinje cell PC layer section that was analyzed and averaged within each animal.

QUANTIFICATION AND STATISTICAL ANALYSIS

Values of n and p values are reported in the figure legends. In all figures, error bars represent ±SEM, *$p < 0.05$, ***$p < 0.001$.

To test for statistical differences between the baseline EPSCs and the EPSC amplitude post-stimulation, used a paired Student's t-test and compared the values for the last 5 min of the baseline recording to those for the last 5 min of the post-stimulation recording.

To test for statistical difference between the change in gain post-stimulation between WT and 4E-BP-KOs, we used a two-tailed Mann–Whitney U-test with a significance set at $p = 0.05$. To conduct the statistical calculations, we used the Mann-Whitney U calculator at https://www.socscistatistics.com/tests/mannwhitney/default2.aspx and compared the values for the last 5 min of the recording for WTs and 4E-BP-KOs.

For calcium imaging, cerebellar morphological analysis and physiological innervation of excitatory inputs onto Purkinje cells, comparisons were made using two-tailed Student's t-test with equal variance.

Cell Reports, Volume *39*

Supplemental information

Loss of 4E-BP converts cerebellar long-term depression to long-term potentiation

Natasha Saviuk, Yumaine Chong, Peng Wang, Sara Bermudez, Zhe Zhao, Arjun A. Bhaskaran, Derek Bowie, Nahum Sonenberg, Ellis Cooper, and A. Pejmun Haghighi

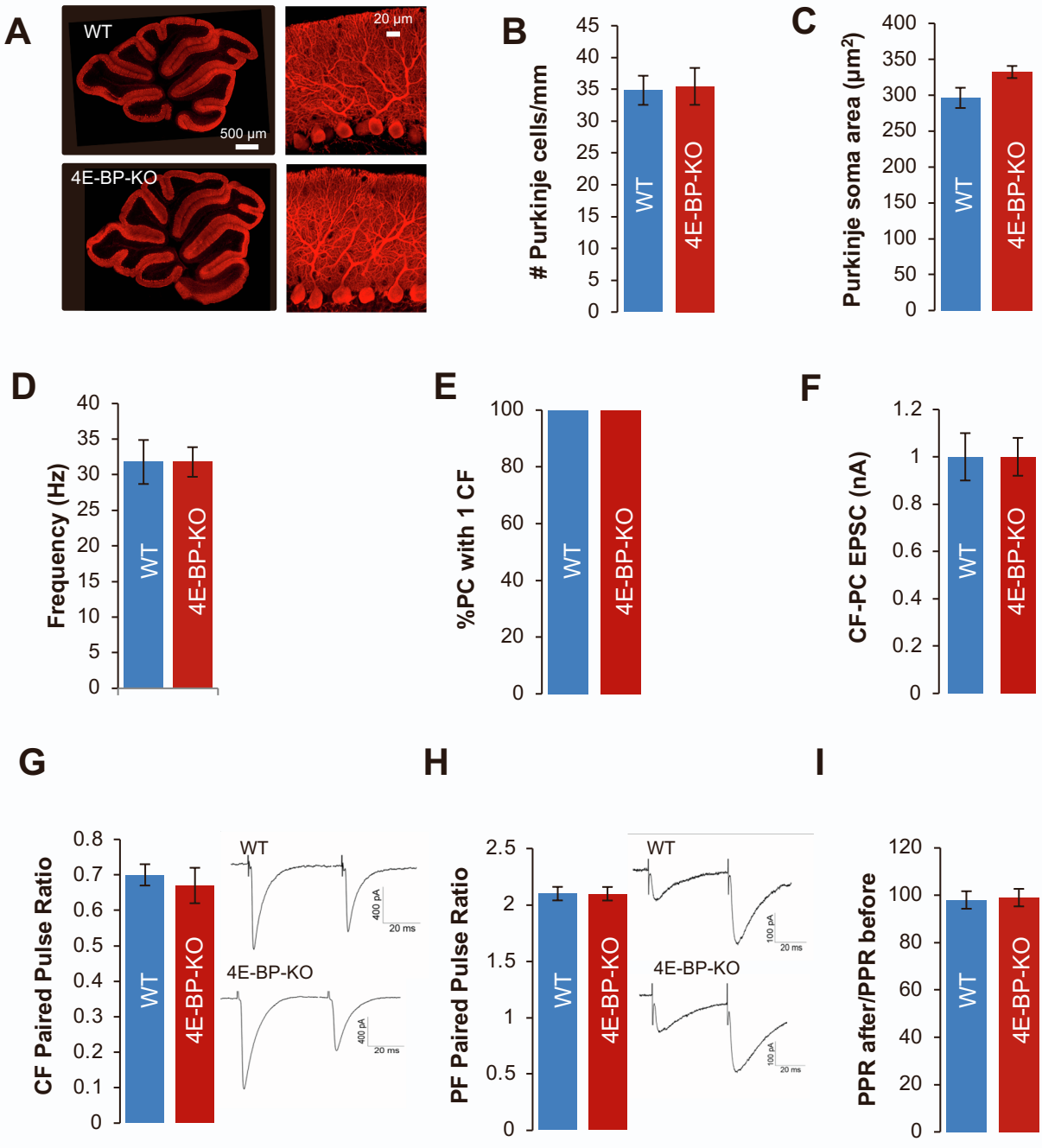
A
WT
500 µm
20 µm
4E-BP-KO
B
Purkinje cells/mm
45
40
35
30
25
20
15
10
5
0
WT
4E-BP-KO
C
Purkinje soma area (µm²)
400
350
300
250
200
150
100
50
0
WT
4E-BP-KO
D
Frequency (Hz)
40
35
30
25
20
15
10
5
0
WT
4E-BP-KO
E
%PC with 1 CF
100
80
60
40
20
0
WT
4E-BP-KO
F
CF-PC EPSC (nA)
1.2
1
0.8
0.6
0.4
0.2
0
WT
4E-BP-KO
G
CF Paired Pulse Ratio
0.8
0.7
0.6
0.5
0.4
0.3
0.2
0.1
0
WT
4E-BP-KO
WT
400 pA
20 ms
4E-BP-KO
400 pA
20 ms
H
PF Paired Pulse Ratio
2.5
2
1.5
1
0.5
0
WT
4E-BP-KO
WT
100 pA
20 ms
4E-BP-KO
100 pA
20 ms
I
PPR after/PPR before
120
100
80
60
40
20
0
WT
4E-BP-KO

Figure S1 The cerebellar anatomy and excitatory synaptic transmission is normal in 4E-BP-KO mice. Related to Figure 1.

A) The gross anatomical structure of cerebella, assessed by staining transverse slices for calbindin 28K (red), is comparable between wild-type mice (top) and in 4E-BP-KO mice (bottom). Scale bar: 500μM, 20μM.

B) There were no statistical differences between WT and 4E-BP-KO cerebella in PC cell density.

C) PCs from WT and 4E-BP-KO cerebella had comparable soma size.

D) Intrinsic firing frequency of PCs in acute slices from 4E-BP-KOs (24.32hz ± 5.09, n=5) compared to WTs (34.10hz ± 6.67 n=4) (two-tailed Student t-test P=0.29)

E) At P21, PCs in both WT (n=9) and 4E-BP-KO (n=10) mice are innervated by a single CF.

F) The amplitude of CF-EPSCs is comparable between WTs (-924.31pA ± 90.01, n= 7) and 4E-BP-KOs (-1011.86pA ± 101.98, n=9) (two-tailed Student t-test P=0.54).

G) CF paired-pulse ratio, measured by giving two pulses 50 ms apart, is not statistically different between WTs (0.70 ± 0.01, n= 9) and 4E-BP-KOs (0.65 ± 0.02, n=10) (two-tailed Student t-test P=0.11).

H) Paired pulse facilitation, measured by giving two pulses 50 ms apart, is comparable between WT (2.09 ± 0.02, n=18) and 4E-BP-KO (2.10 ± 0.02, n=17) mice (two-tailed Student t-test P=0.93).

I) PF paired-pulse ratio before and after applying the LTD inducing protocol is not statistically different in neither WTs (n= 5) nor 4E-BP-KO cerebella (n= 5) (two-tailed Student t-test P=0.42).

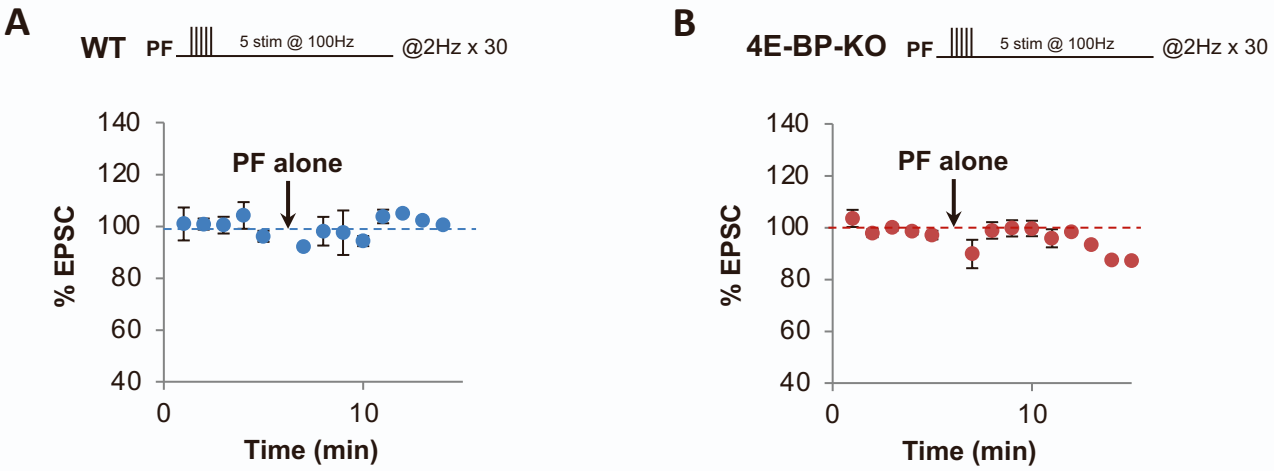

Figure S2. The burst stimulation protocol alone does not cause LTP. Related to Figure 2.

A) In WTs, delivering parallel fibers trains of five pulses at 100 Hz only, leaving out the conjunctive depolarization, resulted in no significant change from baseline (97.17 ± 4.92%, t= 7-11 min, n=4, paired Student t-test P=0.33).

B) in 4E-BP-KOs, delivering parallel fibers trains of five pulses at 100 Hz accompanied without conjunctive depolarization, resulted in no significant change from baseline (96.79 ± 3.82%, t= 7-11 min, n=8, paired Student t-test P=0.36).

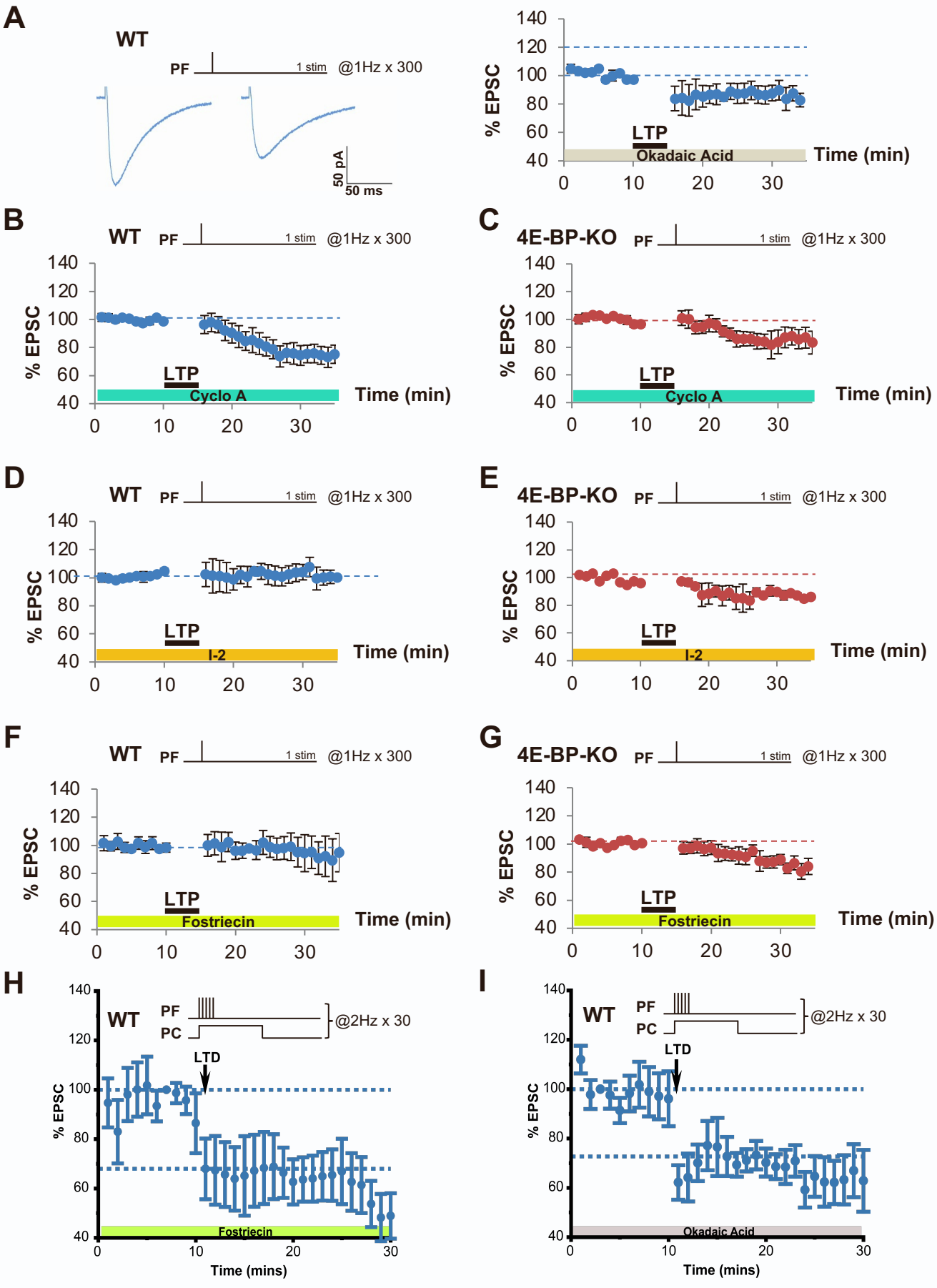
A
WT
PF
1 stim
@1Hz x 300
50 pA
50 ms
% EPSC
LTP
Okadaic Acid
Time (min)
B
WT
PF
1 stim
@1Hz x 300
% EPSC
LTP
Cyclo A
Time (min)
C
4E-BP-KO
PF
1 stim
@1Hz x 300
% EPSC
LTP
Cyclo A
Time (min)
D
WT
PF
1 stim
@1Hz x 300
% EPSC
LTP
I-2
Time (min)
E
4E-BP-KO
PF
1 stim
@1Hz x 300
% EPSC
LTP
I-2
Time (min)
F
WT
PF
1 stim
@1Hz x 300
% EPSC
LTP
Fostriecin
Time (min)
G
4E-BP-KO
PF
1 stim
@1Hz x 300
% EPSC
LTP
Fostriecin
Time (min)
H
WT
PF
PC
@2Hz x 30
LTD
% EPSC
Fostriecin
Time (mins)
I
WT
PF
PC
@2Hz x 30
LTD
% EPSC
Okadaic Acid
Time (mins)

Figure S3. Phosphatase inhibition prevents LTP in WTs and 4E-BP-KO mice. Related to Figure 4.

A) In WTs, pharmacological inhibition of phosphatase activity with the antagonist Okadaic Acid (1mM) blocks LTP induction (n=4).

B) In WTs, pharmacological inhibition of PP1 with I-2 (100 nM) blocks LTP induction (n=4).

C) PP1 inhibition effectively prevents LTP in 4E-BP-KOs (n=3).

D) Pharmacological inhibition of PP2B with the antagonist Cyclosporin A (100mM) completely blocks LTP in WTs and instead induces LTD (n=6).

E) Blocking PP2B in 4E-BP-KOs during LTP induction prevents potentiation (n=5).

F) In WTs, PP2A inhibition using the pharmacological inhibitor Fostriecin (50 nm) blocks LTP (n=5).

G) PP2A inhibitor Fostriecin (50 nm) blocks LTP in 4E-BP-KO slices (n=4).

H) In WTs, LTD remains intact when slices are treated with Okadaic Acid (1mM) (n=4) or **(I)** with specific PP2A inhibitor Fostriecin (50 nm) (n=6).

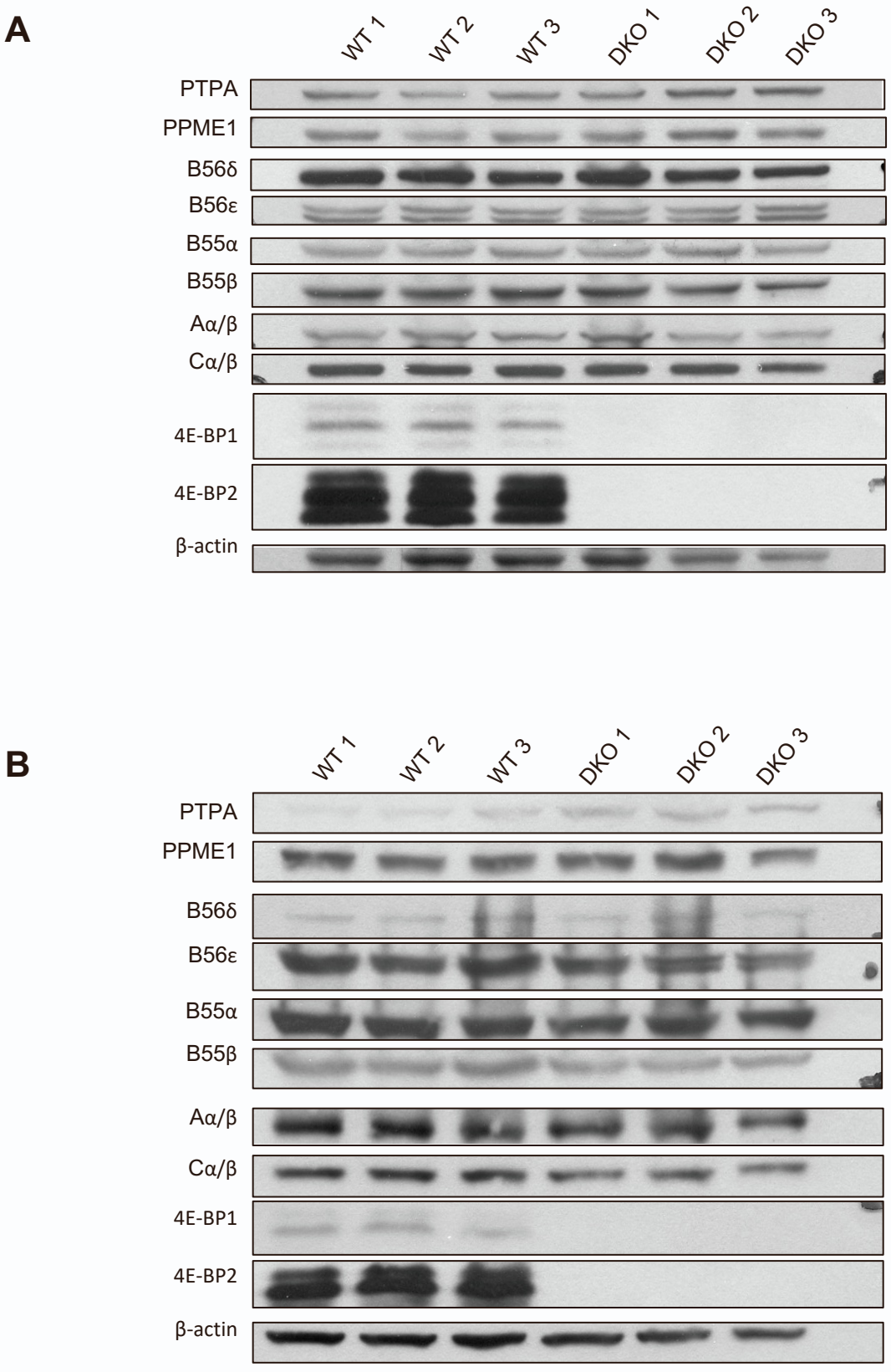
A
WT 1
WT 2
WT 3
DKO 1
DKO 2
DKO 3
PTPA
PPME1
B56δ
B56ε
B55α
B55β
Aα/β
Cα/β
4E-BP1
4E-BP2
β-actin
B
WT 1
WT 2
WT 3
DKO 1
DKO 2
DKO 3
PTPA
PPME1
B56δ
B56ε
B55α
B55β
Aα/β
Cα/β
4E-BP1
4E-BP2
β-actin

Figure S4. PPME1 is not changed in 4E-BP mutant mice. Related to Figure 5

(A)&(B) Additional western blots used for quantifications in Figure 5B in addition to that shown in Figure 5A.